Title

Fluorine-18 incorporation and radiometal coordination in macropa ligands for PET imaging and targeted alpha therapy.

Journal

Chemical Communications, 60(83)

Authors

Kanagasundaram, Thines

Sun, Yang

Lee, Kevin

et al.

Publication Date

2024-10-15

DOI

10.1039/d4cc04165h

Peer reviewed

HHS Public Access

Author manuscript

Chem Commun (Camb). Author manuscript; available in PMC 2024 December 16.

Published in final edited form as:

Chem Commun (Camb). ; 60(83): 11940–11943. doi:10.1039/d4cc04165h.

Fluorine-18 Incorporation and Radiometal Coordination of Macropa Ligands for PET Imaging and Targeted Alpha Therapy†

Thines Kanagasundaram[a], **Yang Sun**[b], **Kevin K. Lee**[a,c], **Samantha N. MacMillan**[a], **Pedro Brugarolas**[b], **Justin J. Wilson**[a,c]

[a]Department of Chemistry and Chemical Biology, Cornell University, Ithaca, NY-14853, USA.

[b]Department of Radiology, Massachusetts General Hospital and Harvard Medical School, Boston, MA-02114, USA.

[c]Department of Chemistry and Biochemistry, University of California Santa Barbara, Santa Barbara, CA-93106, USA.

Abstract

The development of theranostic agents for radiopharmaceuticals based on therapeutic alpha emitters marks an important clinical need. We describe a strategy for the development of theranostic agents of this type via the functionalization of the ligand with the diagnostic radionuclide fluorine-18. An analogue of macropa, an 18-membered macrocyclic chelator with high affinity for alpha therapeutic radiometals, was synthesized and its complexation properties with metal ions were determined. The new macropa-F ligand was used for quantitative radiometal complexation with lead-203 and bismuth-207, as surrogates for their alpha-emitting radioisotopes. As a diagnostic partner, a radiofluorinated macropa ligand was used for quantitative bismuth(III) and lead(II) complexation. All fluorine-18 and radiometal complexes are highly stable in human serum over several days. This study presents a new proof-of-principle approach for developing theranostic agents based on alpha-emitting radionuclides and fluorine-18.

Nuclear medicine uses radioactivity to image and treat diseases, primarily via the use of radiopharmaceuticals.[1] The application of a given radiopharmaceutical depends on the primary emissions of the incorporated radionuclide. Gamma (γ) and positron (β^+) emitters can be used for diagnostic single-photon emission computed tomography (SPECT) and positron emission tomography (PET) imaging, whereas Auger electron, alpha (α), and negatron (β^-) emitters can be leveraged for therapy.[1] In recent years, several therapeutic radiopharmaceuticals have been clinically approved for different indications, including $^{223}RaCl_2$ as Xofigo® (Bayer AG), ^{177}Lu DOTA-TATE as Lutathera® and Lutetium (^{177}Lu) vipivotide tetraxetan as Pluvicto® (both Novartis AG).[2-4] The latter two therapeutic agents benefit from the availability of ^{68}Ga, which can be used in place of ^{177}Lu to enable

†Electronic Supplementary Information (ESI) available: Experimental procedures, NMR spectra, mass spectra, HPLC and TLC chromatograms, X-ray diffraction data. CCDC 2377788. See DOI: 10.1039/x0xx00000x

pbrugarolas@mgh.harvard.edu; justinjwilson@ucsb.edu.

Conflict of Interest

The authors T.K., Y. S. P. B, and J.J.W. are listed as inventors on a patent application related to this work.

diagnostic applications. These so-called theranostic agents can monitor and evaluate radiotherapeutic treatment afforded by ^{177}Lu via PET imaging of the ^{68}Ga nuclide.[1, 5] This concept facilitates clinical approval by providing an accurate means of assessing dosimetry and patient response. However, the development of theranostic agents requires that the therapeutic radionuclide has a radioisotope that is suitable for imaging and can label the same radiopharmaceutical agent. In this context, there have been significant challenges in identifying suitable diagnostic partner radionuclides for α-emitting therapeutic nuclides like ^{212}Pb ($t_{1/2}$ = 10.6 h), ^{212}Bi ($t_{1/2}$ = 60.6 min), ^{213}Bi ($t_{1/2}$ = 45.6 min), and ^{225}Ac ($t_{1/2}$ = 10 d).[6-8] In particular, the large ionic radii of these radiometals often require coordination chemistry approaches for radiolabelling that are distinct from conventional smaller diagnostic radiometals like ^{64}Cu, ^{68}Ga, and ^{111}In. Consequently, there is a need to develop approaches to access theranostic α-emitting radiopharmaceuticals.[5, 9-12] One approach to minimize the mismatch of diagnostic and therapeutic radiopharmaceuticals is to directly incorporate the widely available ^{18}F PET isotope ($t_{1/2}$ = 110 min; β^+_{max} = 0.635 MeV) on the same chelator.[1] Previous examples include the use of [^{18}F]M-F or the use of ^{19}F/^{18}F isotopic exchange reactions on pendent arms.[13-18] In this work, we wanted to go one step further by incorporating ^{18}F directly into the chelator backbone thus minimizing the structural footprint and its effect on its pharmacology. The new ligand, **[^{18}F]macropa-F**, is an analogue of the 18-membered macrocyclic chelator **macropa** and can be used for metal complexation.[19] In parallel to this, the non-radioactive fluorine-containing **macropa-F** was labelled with ^{203}Pb and ^{207}Bi, analogues of their alpha-emitting radioisotopes ^{212}Pb and $^{212/213}$Bi. Finally, the stabilities of the new radioactive complexes were analysed in human serum, validating this approach for the development of new α-emitting radiotheranostic agents.

The **macropa-Me$_2$-NO$_2$** precursor was targeted because of the high affinity of **macropa**-like chelators for α-emitters, as well as the known susceptibility of aromatic nitro compounds to radiofluorination reactions.[20, 21] The synthesis of **macropa-Me$_2$-NO$_2$** is shown in Scheme 1. The picolinic-acid methyl ester functionalized crown ether **1** was alkylated with the mesylated picolinic acid methyl ester **2** to obtain the analytically pure and **macropa-Me$_2$-NO$_2$** with a yield of 37% after column chromatography and high-performance liquid chromatography (HPLC).[22-24] In addition, the fluorine-containing analogue **macropa-F** was synthesized.

This compound was targeted because it could be used as a non-radioactive surrogate of the ^{18}F-labelled version and for the complexation of the alpha emitters. **Macropa-F** was synthesized in two steps, using the fluorinated picolinic pendent arm **3**, and it was obtained in high purity after reversed-phase chromatographic purification. With **macropa-F** in hand, we sought to investigate how the fluorine substituent in the picolinate pendent donor would affect metal ion coordination. Given the relevance of ^{212}Pb and ^{213}Bi for alpha therapy, the complexation properties of this ligand with Pb^{2+} and Bi^{3+} were investigated with ^{1}H NMR spectroscopy and high-resolution electrospray ionization mass spectrometry (HR-ESI-MS). The NMR spectra of **macropa-F** in the presence of Bi^{3+}, Pb^{2+}, and La^{3+}, a surrogate for ^{225}Ac, in an aqueous solution at pH = 7 are shown in Figures 1 and S2 (ESI†). Consistent with prior NMR studies on **macropa** complexes, the NMR spectra of **macropa-F** with these

metal ions show significant changes in the chemical shifts upon coordination. For example, the benzylic methylene proton signals split into two doublets, consistent with complex formation.[25] Further, complex formation was verified by HR-ESI-MS measurements, which displays the expected *m*/*z* molecular ion peaks for the complexes. Notably, the molecular ion peak for the $[M+H]^+$ ion of **[Pb(macropa-F)]** at *m*/*z* = 757.2119 showed the characteristic isotopic pattern arising from the naturally abundant isotopes ^{204}Pb, ^{206}Pb, ^{207}Pb, and ^{208}Pb (Figure S60, ESI†). A crystal structure of **[Bi(macropa-F)]$^+$** was also obtained (Figure 2). Compared to the previously reported crystal structure of **[Bi(macropa)]$^+$**,[25] that of **[Bi(macropa-F)]$^+$** is very similar. The coordination geometry of the Bi(III) ion can best be described as a six-coordinate pentagonal pyramid. This asymmetric geometry is most likely a consequence of the stereochemically active $6s^2$ lone pair, which occupies the axial position of a pentagonal bipyramid. Importantly, the interatomic distances between the Bi(III) ion and the ligand donor atoms within **[Bi(macropa-F)]$^+$** are nearly identical to those found in **[Bi(macropa)]$^+$**, indicating that the F atom does not negatively alter the coordination properties of this ligand (Table S2, ESI†).

To validate the ability of **macropa-Me$_2$-NO$_2$** to be radiofluorinated, it was treated with [^{18}F]KF and [2.2.2]cryptand (K_{222}) in DMSO at 130 °C, followed by the addition of an aqueous solution of lithium hydroxide in ethanol (Scheme 1a). Under these conditions, the methyl esters were cleaved, and **[^{18}F]macropa-F** was isolated with a radiochemical yield (RCY) of 20% after semi-preparative HPLC purification. Notably, the esters, as protecting groups, are necessary for ^{18}F radiolabelling; the free acid form of this ligand cannot be radiolabelled under these conditions. The subsequent addition of non-radioactive $PbCl_2$ and $Bi(NO_3)_3{\cdot}5H_2O$ salts gave the radiofluorinated metal complexes **[^{18}F][Pb(macropa-F)]** and **[^{18}F][Bi(macropa-F)]$^+$** in high radiochemical purity (>95%) after C_{18}-cartridge purification with RCYs of 73% and 57%, respectively. The radio-HPLC chromatograms of the radioactive complexes and the UV-detected HPLC chromatograms of the non-radioactive complexes display peaks corresponding to the major products with equivalent retention times, confirming their chemical identities (Figure 3). To verify the stability of the radiolabelled complexes, they were incubated in human serum at 37 °C for up to 4 h (Table S3, ESI†). Under these conditions, no degradation of the complexes occurs, indicating that radiofluorination of the macrocycle is a suitable approach for generating a stable PET agent in vivo.

Next, we investigated the ability of the modified chelators to bind to therapeutically relevant radiometals. Given the efficacy of **macropa** for the alpha therapeutic radionuclides ^{213}Bi and ^{212}Pb, as well as their short physical half-lives that could be compatible with that of ^{18}F, we considered them for this application.[19, 25] In place of ^{213}Bi and ^{212}Pb, however, we used the longer-lived surrogate radioisotopes ^{203}Pb ($t_{1/2}$ = 51.9 h) and ^{207}Bi ($t_{1/2}$ = 31.6 a), which both decay via electron capture, for investigating radiolabelling and long-term stabilities of the complexes.[26, 27] **Macropa** and **macropa-F** were radiolabelled with ^{203}Pb in ammonium acetate buffer (pH = 7, 1.0 M) and with ^{207}Bi in 2-(*N*-morpholino)ethanesulfonic acid (MES) buffer (pH = 5.53, 0.5 M) at room temperature.[26, 27] As shown in Figure

†Electronic Supplementary Information (ESI) available: Experimental procedures, NMR spectra, mass spectra, HPLC and TLC chromatograms, X-ray diffraction data. CCDC 2377788. See DOI: 10.1039/x0xx00000x

4, quantitative radiolabelling with both ligands and radiometals is achieved at ligand concentrations as low as 1 μM. Importantly, **macropa-F** performs comparably well to **macropa**, indicating that the F atom functionalization does not negatively impact its ability to bind to radiometal ions. To validate the chemical identities of the ^{203}Pb radiocomplexes formed, HPLC of the non-radioactive and radioactive complexes was carried out, showing nearly identical retention times for both species (Figure S8, ESI†). Incubation of the radiometal complexes **[^{203}Pb][Pb(macropa-F)]** and **[^{207}Bi][Bi(macropa-F)]$^{+}$** (final ligand concentration in buffer: 5 μM) in human serum (190 μL) at 37 °C revealed that these complexes remain >95% intact over the course of 120 h (Figure 4), demonstrating them to be suitably stable for in vivo applications.

Lastly, the water-octanol distribution coefficients (log$D_{7.4}$) of the **macropa** and **macropa-F** complexes were measured to determine their respective lipophilicities. The log$D_{7.4}$ values of **[^{203}Pb][Pb(macropa)]** and **[^{203}Pb][Pb(macropa-F)]** were determined to be −0.78 ± 0.04 and −0.37 ± 0.01, whereas those for **[^{207}Bi][Bi(macropa)]$^{+}$** and **[^{207}Bi][Bi(macropa-F)]$^{+}$** were measured to be −2.09 ± 0.12 and −1.83 ± 0.24. As these data show, the F atom only has a minimal effect on the complex lipophilicity.

In summary, we successfully developed radiofluorinated **[^{18}F]macropa-F** metal complexes that could potentially be applied for PET imaging. In addition, **macropa-F** still enables radiolabelling with radioisotopes of Bi^{3+} and Pb^{2+}, which are therapeutically relevant. These results demonstrate the potential of developing new theranostic agents via the use of ^{18}F-functionalized radiometal chelators. Given the versatility and widespread availability of ^{18}F, this approach could provide access to theranostic radiopharmaceuticals for many different alpha emitters. Further work is needed to validate this strategy. In particular, the development of bioconjugateable versions of **macropa-F** are needed, along with the corresponding in vivo studies, in order to validate the dual use of ^{18}F for PET imaging in conjunction with alpha emitters for therapy.

Supplementary Material

Refer to Web version on PubMed Central for supplementary material.

Acknowledgments

This research was supported by the National Institutes of Biomedical Imaging and Bioengineering of the National Institutes of Health under the award number 2R56EB029259. This research made use of the NMR Facility at Cornell University, which was supported, in part, by the U.S. National Science Foundation under award number CHE-1531632. The ^{203}Pb and ^{207}Bi isotopes used in this research were supplied by the U.S. Department of Energy Isotope Program, managed by the Office of Isotope R&D and Production. T.K. acknowledges the German Academic Exchange Service (DAAD) for a postdoctoral fellowship.

Data Availability

The data supporting this article have been included as part of the ESI.†

References

1. Lewis JS, Windhorst AD and Zeglis BM, Radiopharmaceutical Chemistry, Springer, Cham, Switzerland, 2019.
2. Sgouros G, Bodei L, McDevitt MR and Nedrow JR, Nat. Rev. Drug Discov, 2020, 19, 589–608. [PubMed: 32728208]
3. Benešová M, Schäfer M, Bauder-Wüst U, Afshar-Oromieh A, Kratochwil C, Mier W, Haberkorn U, Kopka K and Eder M, J. Nucl. Med, 2015, 56, 914–920. [PubMed: 25883127]
4. Hennrich U and Kopka K, Pharmaceuticals, 2019, 12, 114. [PubMed: 31362406]
5. Kostelnik TI and Orvig C, Chem. Rev, 2018, 119, 902–956. [PubMed: 30379537]
6. Poty S, Francesconi LC, McDevitt MR, Morris MJ and Lewis JS, J. Nucl. Med, 2018, 59, 878–884. [PubMed: 29545378]
7. Grieve ML and Paterson BM, Aust. J. Chem, 2021, 75, 65–88.
8. Herrero Álvarez N, Bauer D, Hernández-Gil J and Lewis JS, ChemMedChem, 2021, 16, 2909–2941. [PubMed: 33792195]
9. Nelson BJ, Wilson J, Andersson JD and Wuest F, Pharmaceuticals, 2023, 16, 1622. [PubMed: 38004486]
10. Miederer M, Benešová-Schäfer M, Mamat C, Kästner D, Pretze M, Michler E, Brogsitter C, Kotzerke J, Kopka K, Scheinberg DA and McDevitt MR, Pharmaceuticals, 2024, 17, 76. [PubMed: 38256909]
11. Bobba KN, Bidkar AP, Meher N, Fong C, Wadhwa A, Dhrona S, Sorlin A, Bidlingmaier S, Shuere B, He J, Wilson DM, Liu B, Seo Y, VanBrocklin HF and Flavell RR, J. Nucl. Med, 2023, 64, 1076–1082. [PubMed: 37201957]
12. Bailey TA, Mocko V, Shield KM, An DD, Akin AC, Birnbaum ER, Brugh M, Cooley JC, Engle JW, Fassbender ME, Gauny SS, Lakes AL, Nortier FM, O'Brien EM, Thiemann SL, White FD, Vermeulen C, Kozimor SA and Abergel RJ, Nat. Chem, 2021, 13, 284–289. [PubMed: 33318671]
13. Lepage ML, Kuo HT, Roxin A, Huh S, Zhang Z, Kandasamy R, Merkens H, Kumlin JO, Limoges A, Zeisler SK, Lin KS, Bénard F and Perrin DM, ChemBioChem, 2020, 21, 943–947. [PubMed: 31621172]
14. Liu Y, Tang H, Song T, Xu M, Chen J, Cui X-Y, Han Y, Li Z and Liu Z, Eur. J. Nucl. Med. Mol. Imaging, 2023, 50, 2636–2646. [PubMed: 37103565]
15. Yang T, Peng L, Qiu J, He X, Zhang D, Wu R, Liu J, Zhang X and Zha Z, Eur. J. Nucl. Med. Mol. Imaging, 2023, 50, 2331–2341. [PubMed: 36864362]
16. Whetter JN, Śmiłowicz D and Boros E, Acc. Chem. Res, 2024, 57, 933–944. [PubMed: 38501206]
17. Zhang K, Feng W, Mou Z, Chen J, Tang X and Li Z, Chem. Eur. J, 2023, 29, e202300248. [PubMed: 37102671]
18. Sire C, Meneyrol V, Saffon-Merceron N, Terreno E, Garello F, Tei L, Jestin E, Tripier R and Troadec T, Chem. Sci, 2024, 15, 13550–13557. [PubMed: 39183922]
19. Thiele NA, Brown V, Kelly JM, Amor-Coarasa A, Jermilova U, MacMillan SN, Nikolopoulou A, Ponnala S, Ramogida CF, Robertson AK, Rodríguez-Rodríguez C, Schaffer P, Williams C Jr., Babich JW, Radchenko V and Wilson JJ, Angew. Chem. Int. Ed. Engl, 2017, 56, 14712–14717. [PubMed: 28963750]
20. Jacobson O, Kiesewetter DO and Chen X, Bioconjugate Chem., 2015, 26, 1–18.
21. Basuli F, Zhang X, Brugarolas P, Reich DS and Swenson RE, J. Label. Compd. Radiopharm, 2018, 61, 112–117.
22. Lengacher R, Cosby AG, Śmiłowicz D and Boros E, Chem. Commun, 2022, 58, 13728–13730.
23. Lamarque L, Zwier J and Bourrier E, USA Patent, US 2020/0140413 Al, 2020.
24. Kretschmer J, Chiaffarelli R, Cotton J, Blahut J, Ráliš J, Dračínský M, Matějková S, Vuozzo M, Seeling U, Schmid AM, Martins AF and Polasek M, Angew. Chem. Int. Ed. Engl, 2024, DOI: 10.1002/anie.202409520, e202409520. [PubMed: 39058684]
25. Fiszbein DJ, Brown V, Thiele NA, Woods JJ, Wharton L, MacMillan SN, Radchenko V, Ramogida CF and Wilson JJ, Inorg. Chem, 2021, 60, 9199–9211. [PubMed: 34102841]

26. McNeil BL, Robertson AK, Fu W, Yang H, Hoehr C, Ramogida CF and Schaffer P, EJNMMI Radiopharm. Chem, 2021, 6, 1–18. [PubMed: 33411034]

27. Wilson JJ, Ferrier M, Radchenko V, Maassen JR, Engle JW, Batista ER, Martin RL, Nortier FM, Fassbender ME, John KD and Birnbaum ER, Nucl. Med. Biol, 2015, 42, 428–438. [PubMed: 25684650]

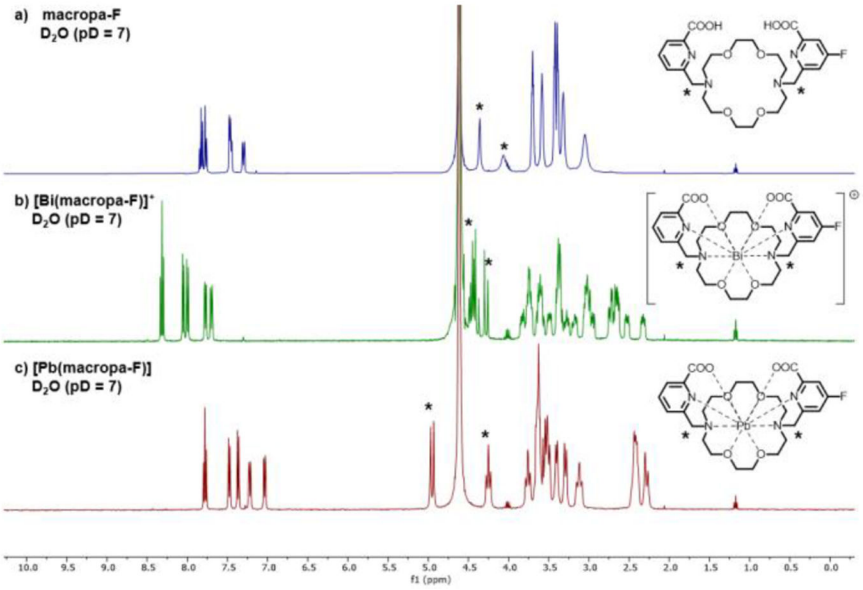

Figure 1:

^{1}H NMR spectra (400 MHz, 298 K, D_2O, pD = 7, MeCN as internal reference) of a) **macropa-F**, b) **[Bi(macropa-F)]$^{+}$**, and c) **[Pb(macropa-F)]**. The diagnostic aliphatic resonances are labelled with asterisks for each compound and indicate the diastereotopic benzylic methylene linker protons.

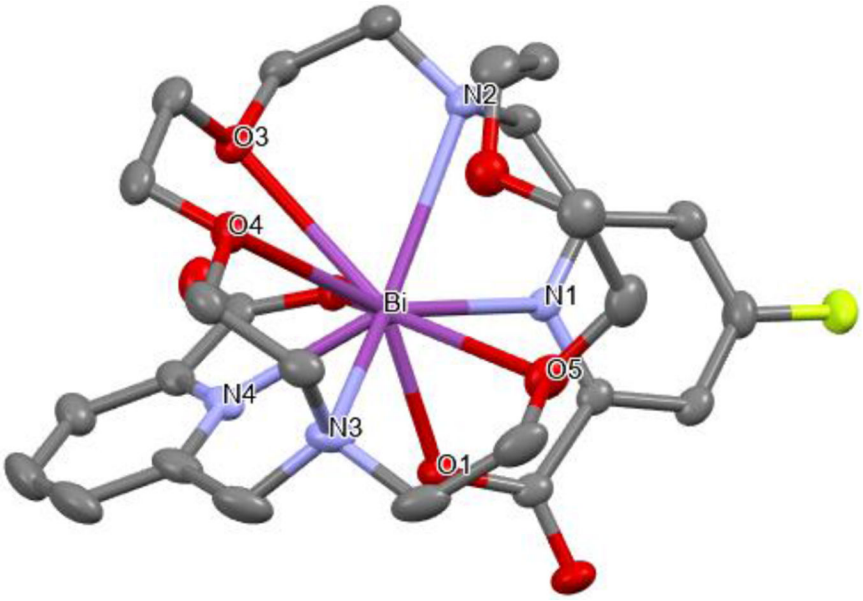

Figure 2:

X-ray crystal structure of **[Bi(macropa-F)]$^{+}$**. Ellipsoids are drawn at the 50% probability level. Hydrogen atoms, counter ions, and solvent molecules are excluded for clarity. Grey = C, red = O, yellow = F, blue = N, purple = Bi.

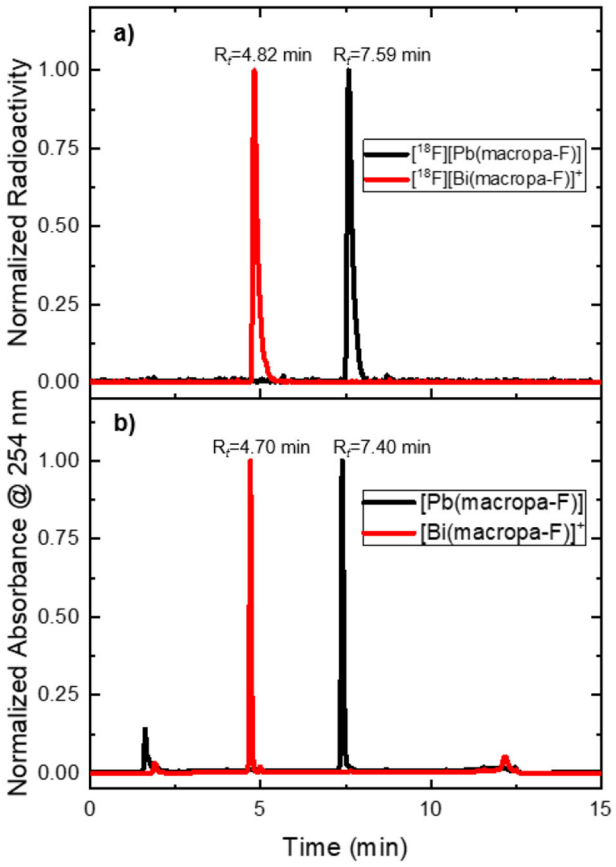

Figure 3:

a) Normalized radio-HPLC traces of the independently injected radiofluorinated complexes **[^{18}F][Pb(macropa-F)]** and **[^{18}F][Bi(macropa-F)]$^+$**. b) Analytical HPLC traces of the independently injected non-radioactive reference metal complexes **[Pb(macropa-F)]** and **[Bi(macropa-F)]$^+$** for comparison.

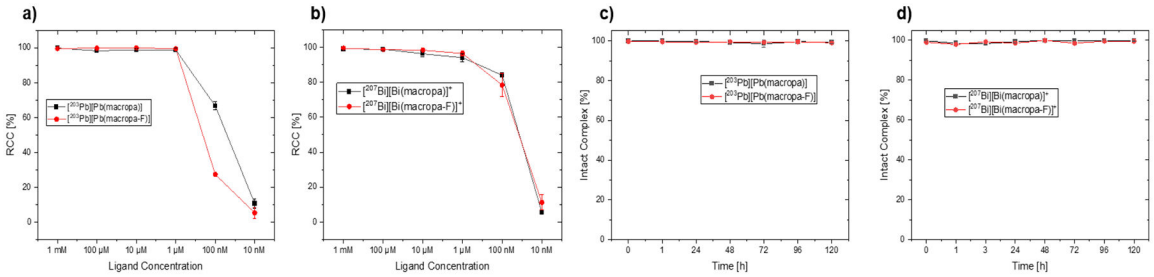

Figure 4:

Summary of the radiolabelling efficiency experiments and kinetic stability studies of **macropa** and **macropa-F** with ^{203}Pb and ^{207}Bi. Experiments were performed in triplicate. a)/b) Concentration-dependent radiolabelling studies with different concentrations of **macropa** and **macropa-F** and ^{203}Pb or ^{207}Bi. c) Human serum stability studies of **[^{203}Pb][Pb(macropa)]** and **[^{203}Pb][Pb(macropa-F)]** complexes at different time points. d) Human serum stability studies of **[^{207}Bi][Bi(macropa)]$^{+}$** and **[^{207}Bi][Bi(macropa-F)]$^{+}$** complexes at different time points.

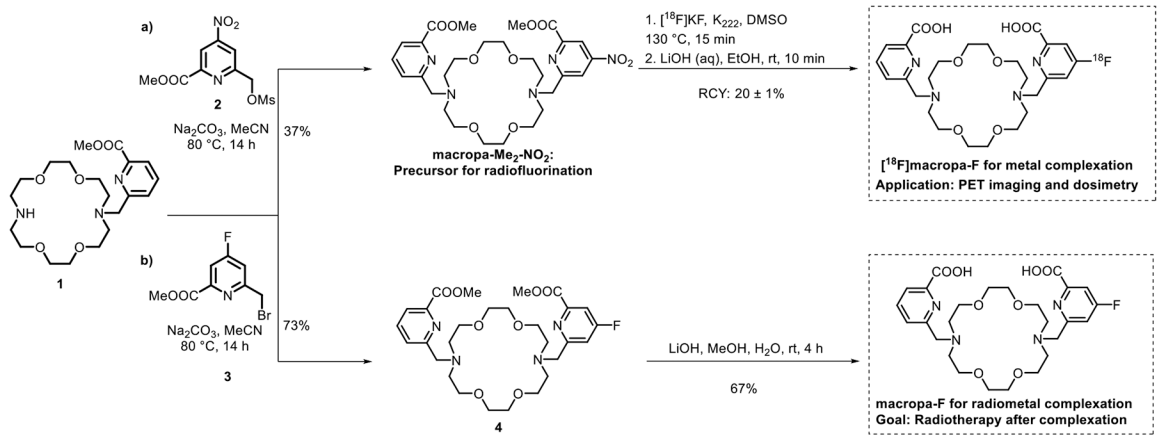

Scheme 1:

a) Synthesis route of a **macropa**-derived precursor **macropa-Me_2-NO_2** for fluorine-18 radiolabelling and b) synthesis of the corresponding non-radioactive reference **4** and **macropa-F** for radiometal complexation.